Progress In Electromagnetics Research M, Vol. 120, 1–14, 2023

Impact of Phase Noise on Sidelobe Cancellation System Utilizing Distributed Phase-Lock-Loops

Qing Wang*, Kang Luo, and Huanding Qin

Abstract—Phase noise is a common hardware impairment that affects the performance of beamforming systems. Therefore, analysis of its impact is of great practical interest. Although Sidelobe Cancellation (SLC) is a mature technique, existing analyses typically ignore the effect of phase noise, due to the shared assumption that the down-conversion circuits have a common local-oscillator (LO). However, when distributed phase-lock-loops (PLLs) are used, the impact of phase noise cannot be neglected. Therefore, this paper derives new mathematical models of performances, including signal-to-interference-plus-noise ratio (SINR) and beamforming gain. Exact and approximated analytical models are obtained, respectively. In addition, we propose an average beam pattern formula to replace the traditional beam pattern formula, to improve the consistency between beam null depth and the beamforming gain. The theoretical findings are verified through signal-level simulations.

1. INTRODUCTION

Sidelobe cancellation (SLC) is a beamforming technique to suppress interference in radio systems that employ high-gain antennas [1, 2]. It is commonly used to mitigate interference, such as that from terrestrial communication systems, in satellite communication (SATCOM) earth stations [3, 4]. To perform beamforming in the digital domain, the received radiofrequency (RF) signals must first be downconverted into an intermediate frequency (IF) band or baseband and then sampled by Analog to Digital Converters (ADCs). The down-conversion (D/C) process unavoidably introduces phase noise from the local-oscillators (LOs), which distort the IF signals by introducing random phase shifts. This distortion reduces the signal-to-noise ratio (SNR) of the received signal and impairs beamforming performance. Therefore, comprehending and quantitatively analyzing the impact of phase noise will significantly aid in practical design.

The purpose of this paper is to investigate how phase noise affects interference cancellation performance in an SLC system that employs a distributed auxiliary array (DAA) and distributed phase-lock loops (PLLs) for the use in SATCOM earth stations. To the best of our knowledge, this subject has not yet been explored. It is worth noting that we are focusing on DAA with distributed PLLs instead of conventional co-located auxiliary arrays (CAAs) with a common PLL. There are two-fold motivations:

First, DAA is preferred over traditional SLC systems that use a CAA due to its advantages such as enhanced spatial resolution, flexibility in deployment, and less vulnerability to line-of-sight blockage. The same advantage has led to the development of distributed beamforming techniques in cellular communications [5, 6]. Unlike CAA, the interantenna spacing in a DAA is typically much larger than a wavelength, often several meters, resulting in significant spatial separation between auxiliary antennas.

Second, the utilization of distributed phase-lock loops (PLLs) is essential in implementing DAA. When utilizing distributed PLLs, each auxiliary antenna is equipped with an individual D/C circuit, and

Received 6 July 2023, Accepted 30 September 2023, Scheduled 14 October 2023

* Corresponding author: Qing Wang (qingwang23@nue.edu.cn).

The authors are with the National Key Laboratory of Electromagnetic Energy, Naval University of Engineering, Wuhan 430033, China.

a common reference PLL is employed to generate the LO signal. Using distributed PLLs is advantageous for DAA because it is more feasible to distribute low-frequency reference signals than high-frequency LO signals, when antenna spacing is large [7, 8]. On the contrary, previous studies have mainly utilized a common PLL that is primarily applicable to CAA.

Many studies on SLC system analysis assume or imply a D/C architecture with a common LO, as seen in [1, 2, 4, 9, 10]. Although a recent study [11] examined the impact of phase noise, its primary focus was on analyzing the beamforming pattern. In addition, their system configuration differs significantly from ours in that they used a simplified one-dimensional linear antenna array, considered only one auxiliary antenna and a single jammer, and assumed the auxiliary channel to be free from phase noise. On the other hand, our recent study [12] focused on a simplified system that only had one auxiliary antenna but took into account the phase noise in the auxiliary channel. The limitation of [12] lies in its derivation in the frequency domain, which hinders its extension to more complex configurations involving multiple auxiliary antennas and interferers.

There is rich literature that focuses on modeling and analysis of the impact of phase noise on MIMO systems, including regular MIMO, e.g., [13–15], massive MIMO and cell-free MIMO, e.g., [7, 16–21]. For regular MIMO, which refers to MIMO with a small number of antennas, a shared LO at the base station is usually considered due to the small array size [13]. Therefore, the main research focus is on inter-symbol-interference (ICI) and common-phase error (CPE), rather than the beamforming performance. The major concern in massive MIMO and cell-free MIMO systems is the impact of phase noise on beamforming with tiled array or arrays [18]. A tiled array is composed of identical elements, in contrast to the SLC system which comprises a high-gain antenna and an array of low-gain auxiliary elements. Additionally, our focus on uncontrollable interference, whether intentional or unintentional, distinguishes our work from current studies that primarily address controllable inter-user and/or inter-cell interference. The differences between SLC systems and other systems require the development of new models that can accurately capture their unique features.

Our paper makes three contributions. Firstly, we establish a mathematical model for SLC system with DAA and distributed PLLs. Secondly, we present new exact and approximated formulas for signal-to-interference-plus-noise ratio (SINR) and beamforming gain. Thirdly, we propose an average beam pattern formula to improve consistency between beam null depth and beamforming gain.

2. SIGNAL MODEL AND PERFORMANCE ANALYSIS

2.1. Signal Model

Consider an SLC system illustrated in Figure 1, in which the main antenna is a high-gain antenna (e.g., a parabolic antenna), and the auxiliary array has an arbitrary geometry and consists of low-gain elements. The received RF signals of the main antenna and auxiliary antennas are downconverted to baseband using independent downconverters which are deployed close to the antennas. The downconverters have separate PLLs for generating the LO signals, while the PLLs are synchronized with a common reference clock signal.

The received signal of the main antenna is

$$d = (g_{\mathrm{s}} s + \mathbf{g}_{\mathrm{c}} \mathbf{c})\, e^{j\varphi_m} + n_m \tag{1}$$

where s is the signal-of-interest (SOI), $\mathbf{c} = [c_k]_{K\times 1}$ the signal vector of the K interferers, n_m the additive white Gaussian noise (AWGN) of main antenna, g_s the gain of the main antenna to the SOI, $\mathbf{g}_c = [g_{c,k}]_{1\times K}$ the gain vector of the main antenna to the interferers, and φ_m the phase noise of the PLL of the main antenna.

Similarly, the received signal of the auxiliary array is

$$\mathbf{x} = (\mathbf{a}_s s + \mathbf{A}_{\mathrm{c}} \mathbf{c}) \odot \phi + \mathbf{n}_x \tag{2}$$

where $\mathbf{n}_x = [n_{x,k}]_{N\times 1}$ is the AWGN vector of the auxiliary array; $\mathbf{a}_s$ is the auxiliary array vector of the SOI; $\mathbf{A} = [\mathbf{a}_{\mathrm{c},k}]_{N\times K}$ is composed by the auxiliary array vectors of the K interferers; $\phi = [e^{j\varphi_n}]_{N\times 1}$, and φ_n is the phase noise of the nth auxiliary antenna. Due to the distributed PLLs, the phase noises of the main and auxiliary antennas are mutually independent. In addition, it is typically assumed that

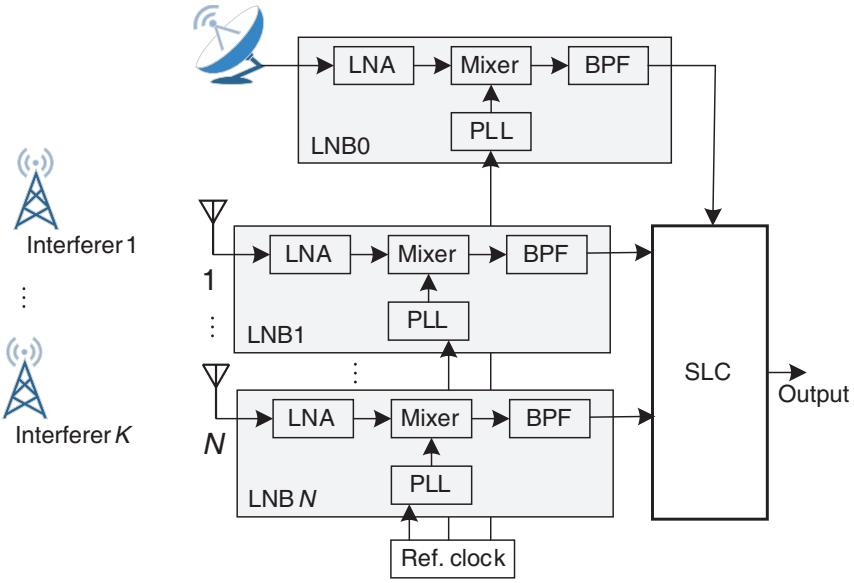

Figure 1. Illustration of SLC system with distributed PLLs.

φ_n is Gaussian. We also assume that they follow the same distribution considering that the PLLs are identical [22].

The output of the SLC system is

$$e = d - \mathbf{w}^{\mathrm{H}}\mathbf{x} \tag{3}$$

where $\mathbf{w}$ is the beamforming vector. $\mathbf{w}$ is calculated using the Wiener method, i.e.,

$$\mathbf{w} = \mathbf{R}_{\mathrm{xx}}^{-1}\mathbf{R}_{\mathrm{xd}} \tag{4}$$

where $\mathbf{R}_{\mathrm{xx}} = \mathrm{E}(\mathbf{x}\mathbf{x}^{\mathrm{H}})$, and $\mathbf{R}_{\mathrm{xd}} = \mathrm{E}(\mathbf{x}d^{*})$. By examining Eqs. (1) and (2), we can observe that phase noise causes multiplicative noise via disturbance to the phases of the received signals. This noise effect leads to distortion of the auto-correlation matrix and crosscorrelation vector, causing deviations in the beamforming vector from its ideal state, ultimately resulting in degraded interference cancellation performance.

2.2. Exact Analysis

In this section, we turn to calculate the beamforming output SINR and then obtain the beamforming gain.

Since phase noise φ_m is typically small, we can approximate $e^{j\varphi_m} \approx 1 + j\varphi_m$, which can be obtained by Taylor expansion. Substituting $e^{j\varphi_m} \approx 1 + j\varphi_m$ into Eq. (1), we get

$$d \approx g_{\mathrm{s}}s + g_{\mathrm{s}}s \cdot j\varphi_m + \mathbf{g}_{\mathrm{c}}\mathbf{c}e^{j\varphi_m} + n_m \tag{5}$$

Since the second term $g_{\mathrm{s}}s \cdot j\varphi_m$ is uncorrelated with $g_{\mathrm{s}}s$, it is therefore treated as noise. The received SINR of the main antenna is given by

$$\begin{aligned}
\mathrm{SINR}_{\mathrm{in}} &= \frac{E\left(|g_{\mathrm{s}}s|^2\right)}{E\left(|g_{\mathrm{s}}s \cdot j\varphi_m + \mathbf{g}_{\mathrm{c}}\mathbf{c}e^{j\varphi_m} + n_m|^2\right)} \\
&= \frac{p_s|g_s|^2}{\sum_k p_k|g_{\mathrm{c},k}|^2 + p_s|g_s|^2\mathrm{E}\left(\varphi^2\right) + p_n} \\
&= \frac{p_s|g_s|^2}{\sum_k p_k|g_{\mathrm{c},k}|^2 + p_s|g_s|^2\sigma_\varphi^2 + p_n}
\end{aligned} \tag{6}$$

The last equality is because φ is zero-mean Gaussian with variance σ_φ^2 [16].
We can also get the received SNR of the main antenna as

$$\mathrm{SNR} = \frac{p_s|g_s|^2}{p_s|g_s|^2\sigma_\varphi^2 + p_n} = \frac{1}{\sigma_\varphi^2 + \dfrac{p_n}{p_s|g_s|^2}} \tag{7}$$

As we can see, SNR is upper bounded by $1/\sigma_\varphi^2$, as the SOI power increases to infinity. Similarly, phase noise will also affect the maximum INR of the main and auxiliary antennas. The limiting effect on SNR and INR is the essential reason for the impact on the system performance.

Similarly, the received INR of the main antenna is

$$\mathrm{INR} = \frac{\mathrm{E}\left(\left|\mathbf{g}_\mathrm{c}\mathbf{c}e^{j\varphi_m}\right|^2\right)}{p_n} = \frac{\sum\limits_k p_k|g_{\mathrm{c},k}|^2}{p_n} \tag{8}$$

Note that phase noise does not change interference power. The output signal of the SLC system is

$$\begin{aligned} e &= \left(g_\mathrm{s}s + \mathbf{g}_\mathrm{c}\mathbf{c}\right)e^{j\varphi_m} + n_m - \mathbf{w}^\mathrm{H}\left(\left(\mathbf{a}_s s + \mathbf{A}_\mathrm{c}\mathbf{c}\right)\odot\phi + \mathbf{n}_\mathrm{x}\right) \\ &= g_s s + \mathbf{g}_\mathrm{c}\mathbf{c} + \hat{n}_m - \mathbf{w}^\mathrm{H}\left(\mathbf{a}_s s + \mathbf{A}_\mathrm{c}\mathbf{c} + \hat{\mathbf{n}}_\mathrm{x}\right) \\ &= \left(g_s - \mathbf{w}^\mathrm{H}\mathbf{a}_s\right)s + \left(\mathbf{g}_\mathrm{c} - \mathbf{w}^\mathrm{H}\mathbf{A}_\mathrm{c}\right)\mathbf{c} + \left(\hat{n}_m - \mathbf{w}^\mathrm{H}\hat{\mathbf{n}}_\mathrm{x}\right) \end{aligned} \tag{9}$$

where,

$$\hat{n}_m = \left(g_s s + \mathbf{g}_\mathrm{c}\mathbf{c}\right)j\varphi_m + n_m \tag{10}$$

$$\hat{\mathbf{n}}_\mathrm{x} = \left(\mathbf{a}_\mathrm{s}s + \mathbf{A}_\mathrm{c}\mathbf{c}\right)\odot j\varphi + \mathbf{n}_\mathrm{x} \tag{11}$$

Therefore, the output SINR is

$$\mathrm{SINR}_\mathrm{out} = \frac{p_s\left|g_s - \mathbf{w}^\mathrm{H}\mathbf{a}_s\right|^2}{\sum\limits_k p_k\left|g_{\mathrm{c},k} - \mathbf{w}^\mathrm{H}\mathbf{a}_{\mathrm{c},k}\right|^2 + p_\mathrm{tot}} \tag{12}$$

where $p_\mathrm{tot} = \mathrm{E}(|\hat{n}_m - \mathbf{w}^\mathrm{H}\hat{\mathbf{n}}_\mathrm{x}|^2)$ is the total effective noise power, which is calculated to be

$$\begin{aligned} p_\mathrm{tot} &= p_n\left(1 + \|\mathbf{w}\|^2\right) + \mathrm{E}\left(\left|g_s s\cdot j\varphi_m - \mathbf{w}^\mathrm{H}\mathbf{a}_\mathrm{s}s\odot j\varphi\right|^2\right) + \mathrm{E}\left(\left|\mathbf{g}_\mathrm{c}\mathbf{c}\cdot j\varphi_m - \mathbf{w}^\mathrm{H}\mathbf{A}_\mathrm{c}\mathbf{c}\odot j\varphi\right|^2\right) \\ &= p_n\left(1 + \|\mathbf{w}\|^2\right) + p_s\left(|g_s|^2\sigma_\varphi^2 + \mathbf{w}^\mathrm{H}\left(\mathbf{a}_\mathrm{s}\mathbf{a}_\mathrm{s}^\mathrm{H}\odot\hat{\mathbf{\Phi}}\right)\mathbf{w}\right) + \sigma_\varphi^2\mathbf{g}_\mathrm{c}\mathbf{P}\mathbf{g}_\mathrm{c}^\mathrm{H} + \mathbf{w}^\mathrm{H}\left(\mathbf{A}_\mathrm{c}\mathbf{P}\mathbf{A}_\mathrm{c}^\mathrm{H}\odot\hat{\mathbf{\Phi}}\right)\mathbf{w} \end{aligned} \tag{13}$$

where $\hat{\mathbf{\Phi}} = \mathrm{E}(j\varphi(j\varphi)^\mathrm{H}) = \sigma_\varphi^2\mathbf{I}_N$.

Discussion: We see from Eq. (13) that the signal components due to phase noise are uncorrelated with each other, so they cannot be cancelled out. As a result, the power of these signal components linearly increases with the interference signal power p_k. Even if the correlated terms in Eq. (13) are fully cancelled, the output SINR will still decrease with an increase in p_k. This implies that the uncorrelated signal components set an upper bound for the output SINR.

Next, we turn to derive the beamforming vector $\mathbf{w}$. First, we need to calculate $\mathbf{R}_\mathrm{xx}$ and $\mathbf{R}_\mathrm{xd}$. It is easy to prove that $\mathrm{E}((\mathbf{a}\odot\mathbf{b})(\mathbf{a}\odot\mathbf{b})^\mathrm{H}) = \mathrm{E}(\mathbf{a}\mathbf{a}^\mathrm{H})\odot\mathrm{E}(\mathbf{b}\mathbf{b}^\mathrm{H})$, when $\mathbf{a}$ and $\mathbf{b}$ are independent. Therefore,

$$\mathbf{R}_\mathrm{xx} = \mathrm{E}\left(\left(\mathbf{a}_s s + \mathbf{A}_\mathrm{c}\mathbf{c}\right)\left(\mathbf{a}_s s + \mathbf{A}_\mathrm{c}\mathbf{c}\right)^\mathrm{H}\right)\odot\mathrm{E}\left(\phi\phi^\mathrm{H}\right) + \mathrm{E}\left(\mathbf{n}_\mathrm{x}\mathbf{n}_\mathrm{x}^\mathrm{H}\right) = \bar{\mathbf{R}}_\mathrm{xx}\odot\mathbf{\Phi} + p_n\mathbf{I}_N \tag{14}$$

where p_n is the AWGN noise power, and

$$\bar{\mathbf{R}}_\mathrm{xx} = \mathrm{E}\left(\left(\mathbf{a}_s s + \mathbf{A}_\mathrm{c}\mathbf{c}\right)\left(\mathbf{a}_s s + \mathbf{A}_\mathrm{c}\mathbf{c}\right)^\mathrm{H}\right) = p_s\mathbf{a}_\mathrm{s}\mathbf{a}_\mathrm{s}^\mathrm{H} + \mathbf{A}_\mathrm{c}\mathbf{P}\mathbf{A}_\mathrm{c}^\mathrm{H} \tag{15}$$

in which, p_s is the power of the SOI, and $\mathbf{P} = \mathrm{diag}\{p_1, \ldots, p_K\}$ is a diagonal matrix whose diagonal elements are the power of the K jamming signals. In addition, we can derive that

$$\mathbf{\Phi} = \mathrm{E}\left(\phi\phi^\mathrm{H}\right) = \left[\mathrm{E}\left(e^{j\varphi_m}e^{-j\varphi_n}\right)\right]_{N\times N} \tag{16}$$

We can see that when $m = n$, $\mathrm{E}(e^{j\varphi_m}e^{-j\varphi_n}) = 1$; otherwise, $\mathrm{E}(e^{j\varphi_m}e^{-j\varphi_n}) = \mathrm{E}(e^{j\varphi_m})\mathrm{E}(e^{j\varphi_n})$ because the phase noises are independent. Since the φ is Gaussian, we have

$$\begin{aligned}\mathrm{E}\left(e^{j\varphi}\right) &= \int e^{j\varphi} f(\varphi)\, d\varphi = \int e^{j\varphi} \cdot \frac{1}{\sqrt{2\pi}\sigma} e^{-\frac{\varphi^2}{2\sigma^2}} d\varphi = e^{-\frac{\sigma^2}{2}} \int \frac{1}{\sqrt{2\pi}\sigma} e^{-\frac{\varphi^2}{2\sigma^2}+\mathrm{j}\varphi+\frac{\sigma^2}{2}} d\varphi \\ &= e^{-\frac{\sigma^2}{2}} \int \frac{1}{\sqrt{2\pi}\sigma} e^{-\frac{\left(\varphi-\mathrm{j}\sigma^2\right)^2}{2\sigma^2}} d\varphi = e^{-\frac{\sigma^2}{2}} \end{aligned} \tag{17}$$

Hence, we have

$$\mathrm{E}\left(e^{j\varphi_m}e^{-j\varphi_n}\right) = \begin{cases} 1 & m = n \\ e^{-\sigma_\varphi^2} & m \neq n \end{cases} \tag{18}$$

Substituting Eq. (18) into Eq. (16), we can get

$$\mathbf{\Phi} = \begin{bmatrix} 1 & \dots & e^{-\sigma_\varphi^2} \\ \vdots & \ddots & \vdots \\ e^{-\sigma_\varphi^2} & \dots & 1 \end{bmatrix} \tag{19}$$

which is a symmetric matrix. Substituting Eq. (15) and (19) into Eq. (14), we can then obtain $\mathbf{R}_{\mathrm{xx}}$.

Following the same procedure, we can derive that

$$\mathbf{R}_{\mathrm{xd}} = e^{-\sigma_\varphi^2}(p_{\mathrm{s}} a_{\mathrm{s}} g_s^* + \mathbf{A}\mathbf{P}\mathbf{g}_{\mathrm{c}}^{\mathrm{H}}) = e^{-\sigma_\varphi^2}\overline{\mathbf{R}}_{\mathrm{xd}} \tag{20}$$

where $\overline{\mathbf{R}}_{\mathrm{xd}}$ is the cross-correlation vector when phase noise is not present. Eqs. (14) and (20) can then be used to calculate the beamforming vector $\mathbf{w}$

$$\mathbf{w} = \left(\bar{\mathbf{R}}_{\mathrm{xx}} \odot \mathbf{\Phi} + p_n \mathbf{I}_N\right)^{-1} \cdot e^{-\sigma_\varphi^2}\overline{\mathbf{R}}_{\mathrm{xd}} \tag{21}$$

Phase noise introduces tapering effect on the interference signal auto-correlation matrix $\bar{\mathbf{R}}_{\mathrm{xx}}$, and a scaling effect is imposed on the cross-correlation vector, which forces the beamforming vector to deviate from the ideal.

The above derivations allow us to calculate $\mathrm{SINR}_{\mathrm{in}}$, the received SINR of the main antennas, and $\mathrm{SINR}_{\mathrm{out}}$, the output SINR of the SLC system. We are now ready to derive the beamforming gain of the system.

The beamforming gain is traditionally defined as the gain of SINR, i.e.,

$$G_1 = \mathrm{SINR}_{\mathrm{out}}/\mathrm{SINR}_{\mathrm{in}} \tag{22}$$

However, there are several drawbacks for this measure. First, the gain increases with the interference power. Second, there is usually a minimum SINR or SNR threshold for a practical communication system, which is not considered in the measure. For example, satellite communications typically use QPSK modulation, and a typically required decoding SNR threshold is $3 \sim 5\,\mathrm{dB}$. Hence, we propose to use the following measure

$$G_2 = p_a/p_b \tag{23}$$

where p_b is the solution of $\mathrm{SINR}_{\mathrm{in}}(p) = \rho_{\mathrm{th}}$; p_a is the solution of $\mathrm{SINR}_{\mathrm{out}}(p) = \rho_{\mathrm{th}}$; and ρ_{th} is the decoding SNR threshold.

There could be multiple definitions of the interference signal power p when multiple interferers are present. In this paper, we define $p = p_1 = \ldots = p_k$, i.e., the interference powers are the same. This corresponds to the scenario where multiple interferers are located at the same distance to the victim receiver and use the same transmission power. Other definitions may be used depending on the question at hand.

2.3. Approximated Analysis

To obtain intuitive observations, the aforementioned formulas are rather complex. Hence, in this section, we introduce certain assumptions to simplify the formulas. The major assumptions considered are:

- SNR is low. This is reasonable for SATCOM, of which the SNR received by the main antenna is typically less than 10 dB due to power limitation of the transponders. We can then ignore the SOI received by the auxiliary antennas, as well as the effect of phase noise on SNR. When the SOI power received by the auxiliary array is low, the signal cancellation effect can be ignored [23]. Mathematically, the low SNR regime is defined as $p_s\|\mathbf{a}_s\|^2 \ll p_n$, or SNR $\ll |g_s|^2/\|\mathbf{a}_s\|^2$. Since the main antenna gain is usually tens of dB larger than the auxiliary array gain, the low SNR regime can cover typical SNR range in practice. Unfortunately, when SNR is high, the behavior of the output SINR becomes complex, so a simple approximated formula may not exist.
- The auxiliary array gain is much larger than the sidelobe gain of the main antenna, such that $\|\mathbf{w}\|^2 \ll 1$. Under this assumption, the noise amplification effect can be ignored.
- The correlated components of interference signals can be completely cancelled. Although complete cancellation is not practical, we anticipate that the coherent interference residual will be minimal if the system is designed appropriately. Particularly for this study, one concern is that the beamforming factor is biased due to the distorted auto-correlation matrix and cross-correlation vector. Nonetheless, if the phase noise variance is known exactly, we can compensate the distortions. Specifically, we can obtain the non-distorted $\bar{\mathbf{R}}_{\mathrm{xx}} = \mathbf{R}_{\mathrm{xx}} \oslash \mathbf{\Phi}$, where $\oslash$ is Hadamard division (element-wise), and $\overline{\mathbf{R}}_{\mathrm{xd}} = e^{\sigma_\varphi^2}\mathbf{R}_{\mathrm{xd}}$. Note that this compensation is not used in our simulations. Under this assumption, we can derive that $g_{\mathrm{c},k} \approx \mathbf{w}_{\mathrm{opt}}^{\mathrm{H}}\mathbf{a}_{\mathrm{c},k}$.

We can then obtain the following approximated formulas

$$\mathrm{SINR}_{\mathrm{in}} \approx \frac{p_s|g_s|^2}{\sum_k p_k|g_{\mathrm{c},k}|^2 + p_n} \tag{24}$$

$$\mathrm{SINR}_{\mathrm{out}} \approx \frac{p_s\,|g_s|^2}{p_n + \sum_k p_k\left(|g_{\mathrm{c},k}|^2\,\sigma_\varphi^2 + \mathbf{w}_{\mathrm{opt}}^{\mathrm{H}}\mathbf{a}_{\mathrm{c},k}\mathbf{a}_{\mathrm{c},k}^{\mathrm{H}} \odot \hat{\mathbf{\Phi}}\mathbf{w}_{\mathrm{opt}}\right)} \approx \frac{p_s\,|g_s|^2}{p_n + (K+1)\,\sigma_\varphi^2 \sum_k p_k\,|g_{\mathrm{c},k}|^2} \tag{25}$$

Equation (24) is derived directly from Eq. (6). Based on the assumption that the SNR is low, while the phase noise variance σ_φ^2 is small, we have $p_s|g_s|^2\sigma_\varphi^2 \ll p_n$. Hence, the term $p_s|g_s|^2\sigma_\varphi^2$ in the denominator of Eq. (6) can be ignored, which results in the approximation of Eq. (24). The approximation of the denominator in Eq. (25) is further explained in Appendix A. We note that this approximation exaggerates the power of phase noise-induced components, thus results in an underestimated output SINR. This will help explain the simulation results presented later.

Substituting Eq. (24) and Eq. (25) into Eq. (2), we can get an approximation of G_1 as

$$\tilde{G}_1 \approx \frac{\sum_k p_k|g_{\mathrm{c},k}|^2 + p_n}{(K+1)\,\sigma_\varphi^2 \sum_k p_k\,|g_{\mathrm{c},k}|^2 + p_n} = \frac{\mathrm{INR}+1}{(K+1)\,\sigma_\varphi^2 \cdot \mathrm{INR} + 1} \tag{26}$$

When INR is high, the noise term can be ignored, and we can then derive the approximated maximum beamforming gain as

$$\hat{G}_1 = \frac{1}{(K+1)\,\sigma_\varphi^2} \tag{27}$$

Therefore, the maximum beamforming gain is proportional with the maximum SNR (cf. Eq. (7)) and decreases with the number of interferers. Substituting Eq. (24) and Eq. (25 into Eq. (23), we can get

$$\tilde{G}_2 = \hat{G}_1 = \frac{1}{(K+1)\,\sigma_\varphi^2} \tag{28}$$

2.4. Beam Pattern

Beam pattern is usually used to visualize the performance of beamforming systems. The null depth can be used to indicate the performance. The deeper the nulls are at the interference angles, the better the

performance is. However, we find that beam pattern may be misguiding when phase noises are present. Traditionally, the composite array beam pattern is calculated by

$$f(\theta) = \left| g(\theta) - \mathbf{w}^H \mathbf{a}(\theta) \right|^2 \tag{29}$$

where θ is a vector consisting of azimuth and elevation angles. The problem of Eq. (29) is that it implicitly assumes that the received signals can be added coherently. That is, Eq. (29) is equivalent to $f(\theta) = \mathrm{E}(|g(\theta)s - \mathbf{w}^H \mathbf{a}(\theta)s|^2)$, where $\mathrm{E}(|s|^2) = 1$. This is, however, not valid since the independent phase noises of the circuits induce uncorrelated signal components. If we use Eq. (29), we would anticipate that there will be a beamforming vector that can produce an infinitely deep null, which means that the interferences can be completely cancelled. This is contradictory with Eqs. (12) and (13), which suggest that there will always be residuals due to the uncorrelated signal components induced by phase noises. Hence, beam pattern analysis should consider the impact of phase noise when distributed PLLs are used. To enable beam pattern analysis while phase noise is present, we propose *average beam pattern* defined as

$$\begin{aligned} f(\theta) &= \mathrm{E}\left(\left| g(\theta) \cdot s e^{j\varphi_m} - \mathbf{w}^{\mathrm{H}} \mathbf{a}(\theta) \odot s\phi \right|^2 \right) \\ &= |g(\theta)|^2 + \mathbf{w}^{\mathrm{H}} \left(\mathbf{a}(\theta) \mathbf{a}^{\mathrm{H}}(\theta) \odot \mathbf{\Phi} \right) \mathbf{w} - 2e^{-\sigma_\varphi^2} \mathrm{Re}\left(\mathbf{w}^{\mathrm{H}} \mathbf{a}(\theta) g^*(\theta) \right) \end{aligned} \tag{30}$$

The derivations above take the impact of phase noise as a modulation effect on the received signals. Another view is that the phase noises cause jittering of the beamforming vector elements, such that the beam pattern varies over time. Hence, we define Eq. (30) as the average beam pattern.

3. NUMERICAL RESULTS

In this section, the presented models of SINR, beamforming gain, and beam pattern with phase noise variances are verified with simulations.

3.1. Simulation Setup

The earth station antenna (the main antenna) is a Ku-band Cassegrain parabolic antenna of 0.8 m diameter with a maximum gain of 38 dB. The auxiliary array, distributed around the main antenna, is a uniform circular array (UCA) with $N = 8$ elements and 4 m diameter. The auxiliary antenna elements are identical. Each element is a low-gain antenna with a maximum gain of 7.7 dB and a 3 dB beamwidth of 135 degrees in the azimuth plane. Figure 2 presents the main antenna and auxiliary array gains. The maximum auxiliary gain is 13 dB, thus the low SNR regime is SNR $\ll$ 25 dB. Since the main antenna gain is larger than the auxiliary gain when azimuth is less than ± 5 degrees, we only consider azimuth angles ≥ 6 degrees in the simulations. The SOI is a QPSK modulated signal with a raised cosine filter of roll-off factor of 0.35 and a span of 32 symbols. The jamming signals are band-limited white Gaussian noises with the same bandwidth as the SOI. The other main simulation parameters are listed in Table 1.

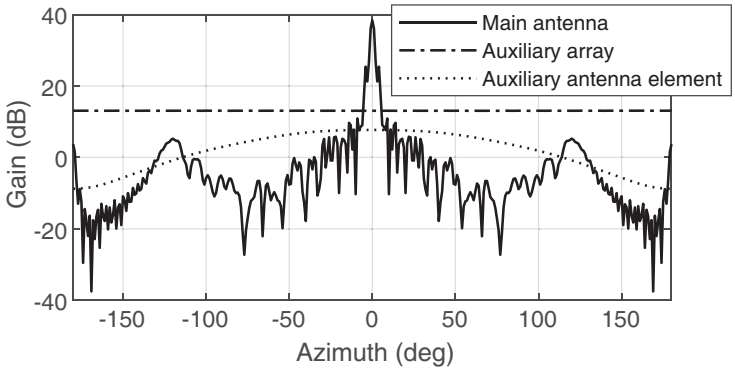

Figure 2. Main antenna and auxiliary array gain comparison.

Table 1. Simulation parameters.

Frequency	12.5 GHz
SOI Azimuth	0 degree
Interferer angles	$\|\theta\| \geq 6$ degrees (sidelobe)
Number of interferers	$1 \sim 3$
Auxiliary array size	8
SNR threshold	3 dB
Bandwidth	1 MHz
Phase noise variance	1e-6 $\sim$ 1e-1 rad^2

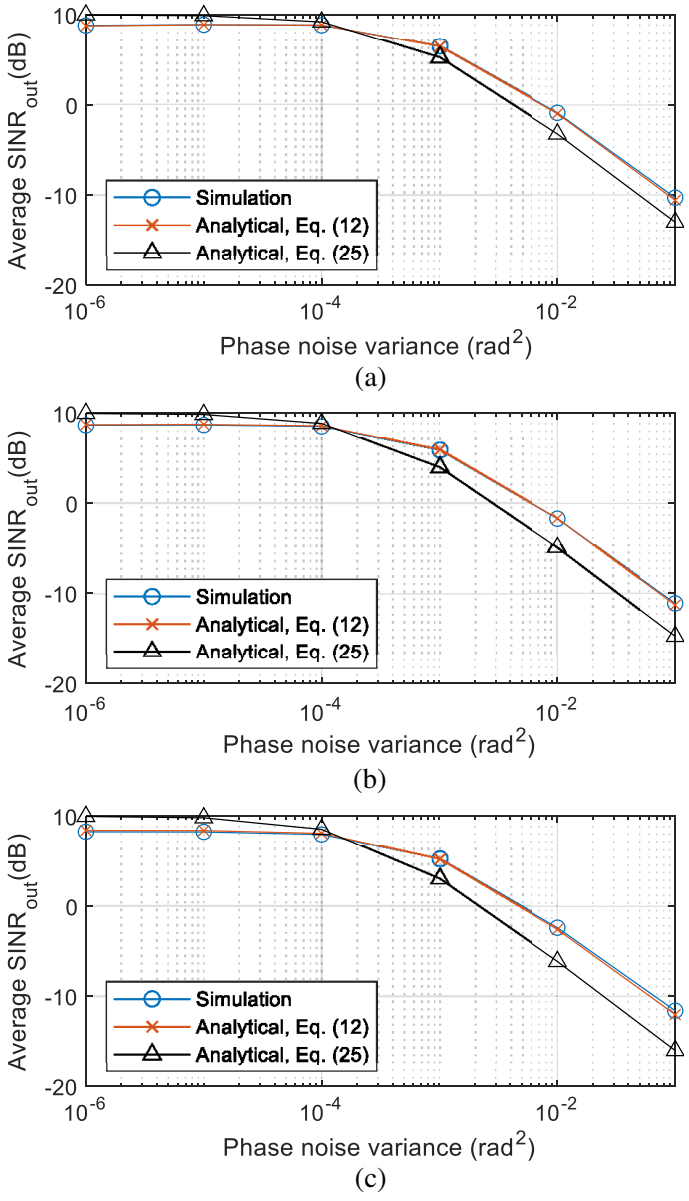

Figure 3. Average output SINR versus phase noise variance. (a) $K = 1$. (b) $K = 2$. (c) $K = 3$.

Note that, in practice, the phase noise variance is around 1e-4 $\sim$ 1e-3 rad^2 in Ku band. Taking Norsat 1008XHBN LNB as an example, which is a popular commercial product that includes a down-conversion circuit using a 10 MHz external reference, and its phase noise level is -75 dBc/Hz@1 kHz, -85 dBc/Hz@10 kHz, and -95 dBc/Hz@100 kHz. The phase noise variance is around 1.6e-3 rad^2 (c.f. [24]). In our numerical simulations, we assume that the phase noise spectrum maintains the same shape as the one given above but is adjusted in magnitude to achieve different levels of phase noise variance. The phase noise impairments can be simulated using the phase noise function in MATLAB.

3.2. SINR Analysis

In this subsection, we compare the output SINR results calculated by Eq. (12) and Eq. (25) with simulation results. We assume INR = 30 dB and SNR = 10 dB. Figure 3 presents the average output SINR versus phase noise variance.

We can see that the error between analytical result of Eq. (12) and simulation results is marginal across various phase noise variances and number of interferers, which confirms the effectiveness of the

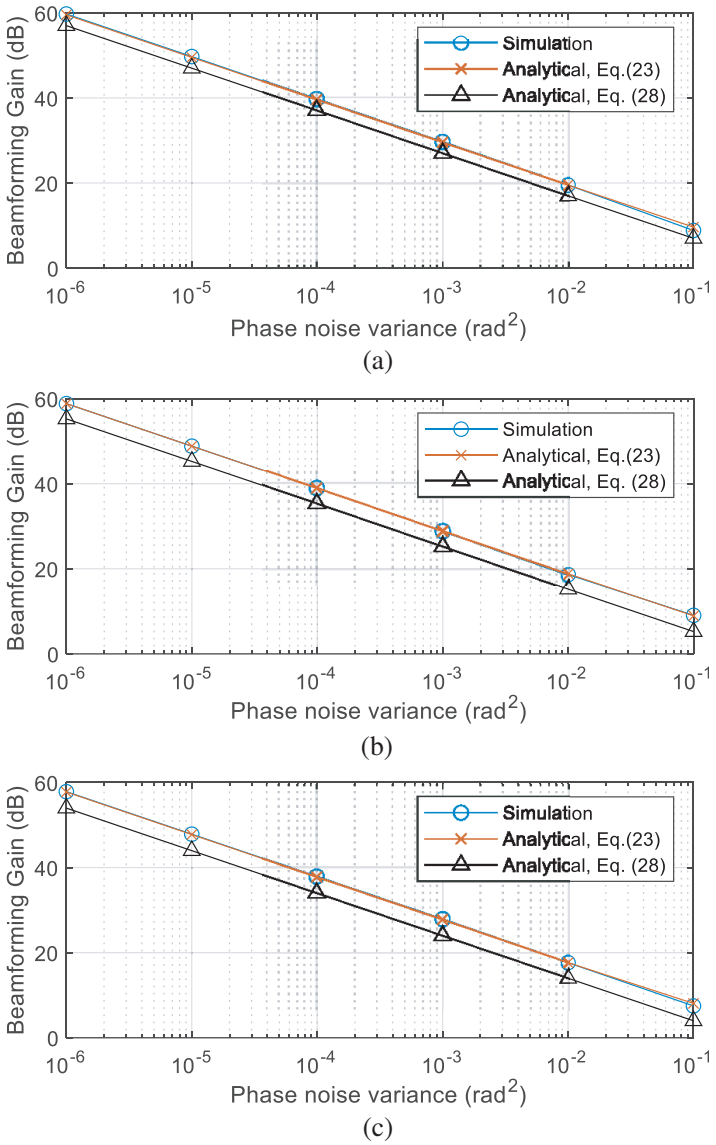

Figure 4. Average beamforming gain versus phase noise variance. (a) $K = 1$. (b) $K = 2$. (c) $K = 3$.

proposed model. The maximum error between analytical and simulation results across all simulated conditions is around 0.4 dB, while SINR decreases monotonically with phase noise variance. Since the INR is fixed at 30 dB, when phase noise variance is less than 1e-3, additive thermal noise has a greater impact on SINR than phase noise. It is noteworthy that despite being based on a set of assumptions, Eq. (25) still provides reliable approximations. However, it tends to underestimate the output SINR when the phase noise variance is low and overestimate it when the variance is high. The error margin reaches its minimum at around 1e-4, which is a typical value in practical applications.

3.3. Beamforming Gain Analysis

In this subsection, we analyze the beamforming gain performance using the mathematical models of Eqs. (23) and (28), and compare with simulation results.

Figure 4 presents the average beamforming gain versus phase noise variance, obtained by Eq. (23) and (28), as well as simulation results. We can see that the analytical results of Eq. (23) tightly approach the simulation results across various phase noise variances and number of interferers. It is also interesting to observe that Eq. (28) can also well approximate Eq. (23) as well as the simulation results, although it is derived upon a number of assumptions. Since Eq. (28) is simple and only related to phase noise variance, it can be used for coarse analysis of the system performance.

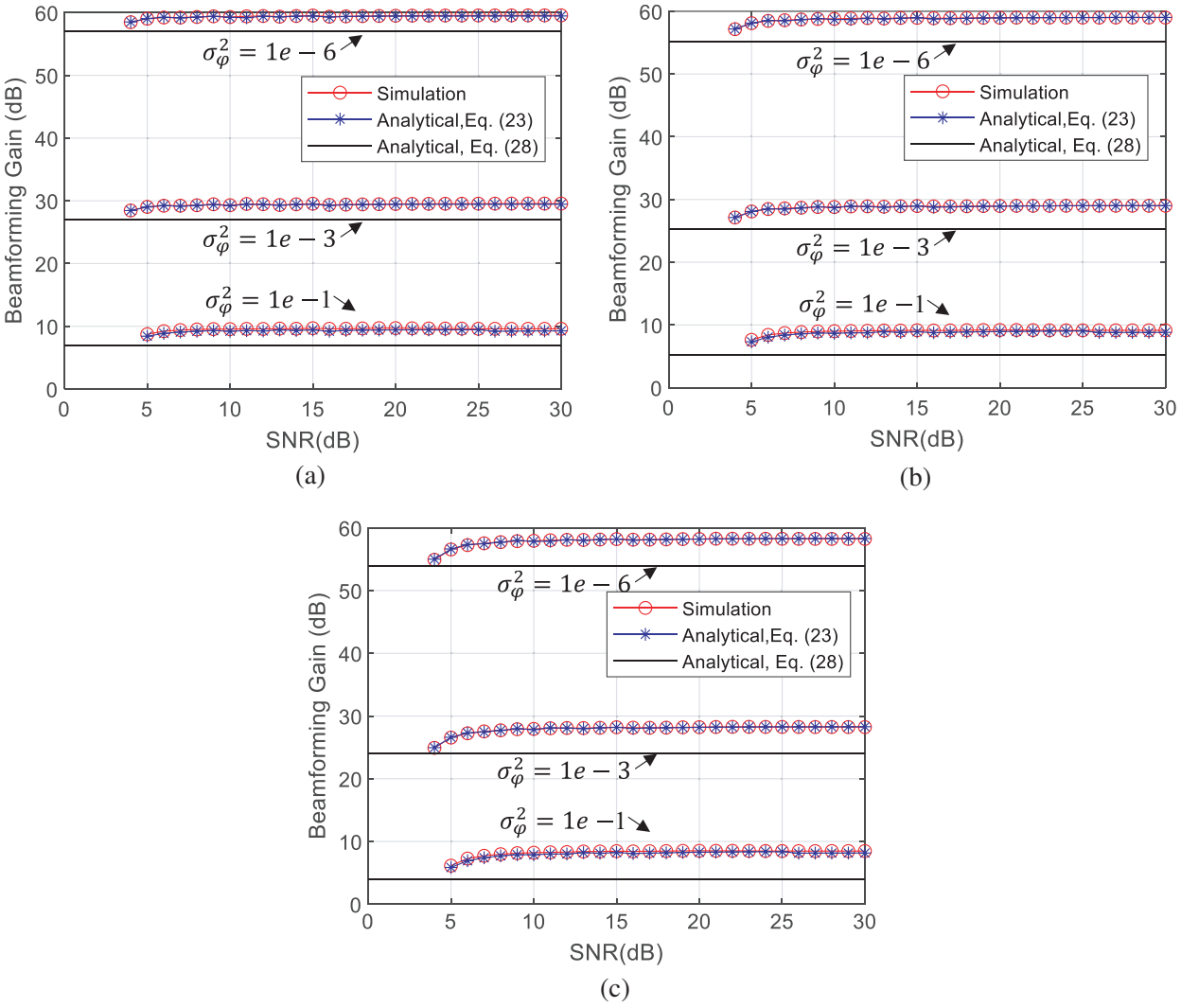

Figure 5. Average beamforming gain versus SNR. (a) $K = 1$. (b) $K = 2$. (c) $K = 3$.

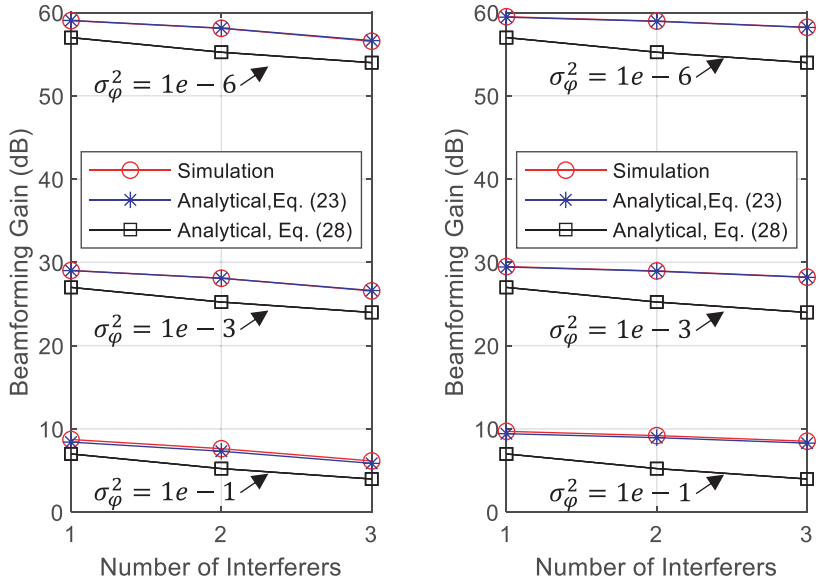

Figure 6. Average beamforming gain versus number of interferers.

Figure 5 presents the average beamforming gain versus SNR for phase noise variances equal to 1e-6, 1e-3, and 1e-1. First, the analytical results provided by Eq. (23) are accurate as evidenced by the alignment of the curves with the simulation results. Second, the approximated formula Eq. (28) also well reflects the beamforming gain performance, though the performance is underestimated by a few decibels. Note that, when SNR is low, say less than 5 dB, no beamforming gain can be realized since the SNR is too low; when SNR is larger than around 25 dB, which violates the low SNR assumption, the signal cancellation effect dominates especially when the phase noise variance is small. Therefore, for these two cases, the errors of Eq. (28) are relatively large.

Figure 6 presents the average beamforming gain versus the number of interferers for various phase noise variances and SNRs. We see that the beamforming gain decreases with the number of interferers. When SNR is low (Figure 6(a)), the curve of Eq. (28) aligns with the simulation results and analytical results of Eq. (23), revealing an accurate approximation. When SNR is high (Figure 6(b)), the effect of SNR is more evident, and the approximation of Eq. (28) is less accurate. Then, the performance predicted by Eq. (28) will become more conservative when the number of interferers increases. When a small number of interferers is concerned, Eq. (28) is still a good performance predictor.

3.4. Beam Pattern Analysis

In this subsection, we compare beam null depth results calculated with traditional beam pattern formula (Eq. (29)) and the proposed average beam pattern formula (Eq. (30)). We assume INR = 30 dB and $K = 1$. The interferer angle is 30 degrees, for which the main antenna gain is 3.4 dB. The beamforming vector is calculated using Eq. (4).

Figure 7 presents an example of the average beam pattern when phase noise variance is 1e-3. We see that the null depth of the average beam pattern at the interferer angle is -25.8 dB, which is much higher than the traditional beam pattern null depth -70.9 dB. According to the null depth of averaged beam pattern, the beamforming gain is around 29.2 dB $(3.4 + 25.8)$, which is in accordance with the results in the last subsection. The traditional formula significantly overestimates the performance.

Figure 8 presents the null depths of traditional and average beam patterns for various phase nose variances. As we can see, the null depth of traditional beam pattern is much lower, while the quantity does not match the beamforming gain obtained in the former subsections. Instead, the null depth of the average beam pattern is proportional to the phase noise variance, coinciding with the beamforming gain. Hence, we suggest using the proposed average beam pattern for performance analysis when distributed PLLs are used.

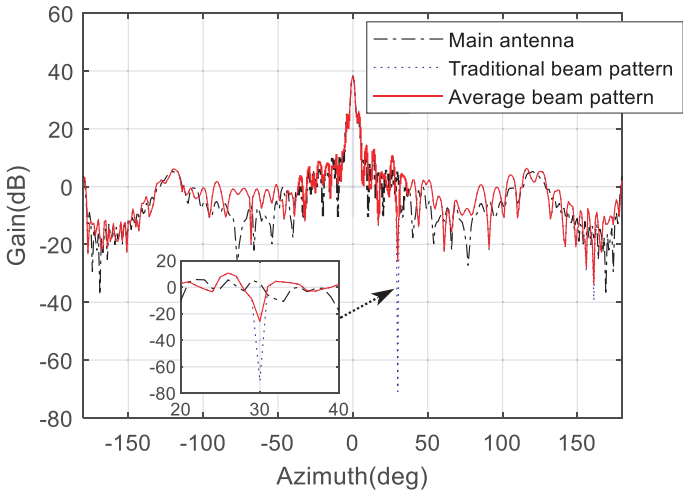

Figure 7. An example of average beam pattern.

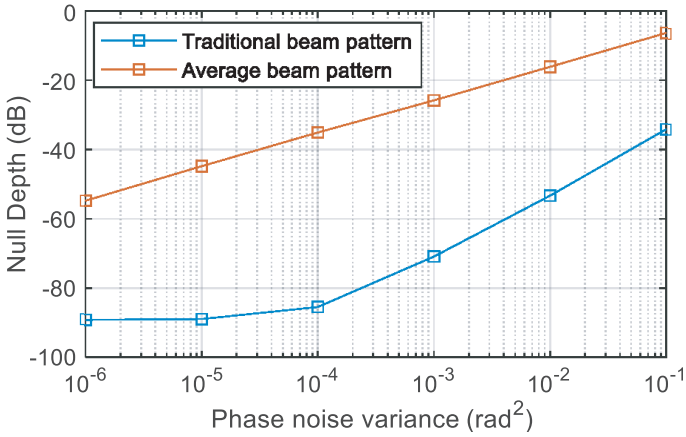

Figure 8. Null depth versus phase noise variance.

4. CONCLUSIONS

This paper presents mathematical models for analyzing the impact of phase noise on the performance of SLC system with DAA and distributed PLLs. Exact and approximate formulas have been derived to calculate beamforming output SINR and beamforming gain. Our findings show that the beamforming gain is inversely proportional to both the phase noise variance and number of interferers. We have proposed an average beam pattern formula that resolves the inconsistency problem between beam null depth and beamforming gain of traditional formulas in the presence of phase noise. The theoretical findings have been validated through simulations.

APPENDIX A.

To make the derivations tractable, we assume that the array vectors of the interferers are mutually orthogonal. Also considering the assumptions in Section 2.3, we can get

$$\mathbf{R}_{\mathrm{xd}} \approx \mathbf{A}_{\mathrm{c}}\mathbf{P}\mathbf{g}_{\mathrm{c}}^{\mathrm{H}} e^{-\sigma_{\varphi}^2} = \bar{\mathbf{A}}_{\mathrm{c}} \left[p_k \left\| \mathbf{a}_{c,k} \right\|^2 \right]_K \mathbf{g}_{\mathrm{c}}^{\mathrm{H}} \tag{A1}$$

$$\mathbf{R}_{\mathrm{xx}} \approx \mathbf{A}_{\mathrm{c}}\mathbf{P}\mathbf{A}_{\mathrm{c}}^{\mathrm{H}} + p_n \mathbf{I}_N = \bar{\mathbf{A}}_{\mathrm{c}} \left[p_k \left\| \mathbf{a}_{c,k} \right\|^2 + p_n \right]_K \bar{\mathbf{A}}_{\mathrm{c}}^{\mathrm{H}} + p_n \mathbf{U}_N \mathbf{U}_N^{\mathrm{H}}$$

where $\bar{\mathbf{A}}_{\mathrm{c}} = [\mathbf{a}_{c,k}/\|\mathbf{a}_{c,k}\|]$, $\mathbf{U}_N$ is orthogonal to $\bar{\mathbf{A}}_{\mathrm{c}}$. The beamforming vector is then approximated as

$$\mathbf{w} \approx \bar{\mathbf{A}}_{\mathrm{c}} \left[\frac{p_k \|\mathbf{a}_{c,k}\|}{p_k \|\mathbf{a}_{c,k}\|^2 + p_n} \right]_K \mathbf{g}_{\mathrm{c}}^{\mathrm{H}} \tag{A2}$$

We can further derive

$$\|\mathbf{w}\|^2 \approx \sum_k \frac{p_k^2 \|\mathbf{a}_{c,k}\|^2 |g_{c,k}|^2}{\left(p_k \|\mathbf{a}_{c,k}\|^2 + p_n\right)^2} \approx \sum_k \frac{|g_{c,k}|^2}{\|\mathbf{a}_{c,k}\|^2} \tag{A3}$$

where the second approximation is due to $p_k\|\mathbf{a}_{c,k}\|^2 \gg p_n$. From Eq. (25) and substituting with Eq. (A3), we derive

$$\begin{aligned} \mathbf{w}_{\mathrm{opt}}^{\mathrm{H}} \mathbf{a}_{\mathrm{c},k} \mathbf{a}_{\mathrm{c},k}^{\mathrm{H}} \odot \hat{\mathbf{\Phi}} \mathbf{w}_{\mathrm{opt}} &= \sigma_\varphi^2 \sum_n |w_{\mathrm{opt},n}|^2 |a_{\mathrm{c},k,n}|^2 \le \sigma_\varphi^2 \|\mathbf{w}_{\mathrm{opt}}\|^2 \|\mathbf{a}_{\mathrm{c},k}\|^2 \\ &\approx \sigma_\varphi^2 \sum_k \frac{|g_{c,k}|^2}{\|\mathbf{a}_{c,k}\|^2} \cdot \|\mathbf{a}_{\mathrm{c},k}\|^2 \approx \sigma_\varphi^2 \sum_k |g_{c,k}|^2 \end{aligned} \tag{A4}$$

To simplify the analysis, we consider the transmission powers of the interferers are equal, therefore,

$$\begin{aligned} \sum_k p_k \left(|g_{\mathrm{c},k}|^2 \sigma_\varphi^2 + \mathbf{w}_{\mathrm{opt}}^{\mathrm{H}} \mathbf{a}_{\mathrm{c},k} \mathbf{a}_{\mathrm{c},k}^{\mathrm{H}} \odot \hat{\mathbf{\Phi}} \mathbf{w}_{\mathrm{opt}} \right) &\approx \sigma_\varphi^2 \sum_k p_k |g_{\mathrm{c},k}|^2 + \sum_k \left(\sigma_\varphi^2 \sum_k p_k |g_{c,k}|^2 \right) \\ &= \sigma_\varphi^2 (K+1) \sum_k p_k |g_{\mathrm{c},k}|^2. \end{aligned} \tag{A5}$$

This explains the approximation of Eq. (25).

REFERENCES

1. Wang, X., W. Zhai, and A. Farina, "A unified framework of adaptive sidelobe canceller design by antenna/subarray selection," *Signal Processing*, Vol. 189, 1–14, 2021.
2. Mohammed, J. R. and K. H. Sayidmarie, "Performance evaluation of the adaptive sidelobe canceller system with various auxiliary configurations," *International Journal of Electronics and Communications*, Vol. 89, 179–185, 2017.
3. Kaitsuka, T. and T. Inoue, "Interference cancellation system for satellite communication earth station," *IEEE Transactions on Communications*, Vol. 32, No. 7, 796–803, 1984.
4. Wang, Q., Y. Li, K. Luo, Q. Wang, F. He, and B. Li, "Auxiliary antenna array analysis and design for sidelobe interference cancellation of satellite communication system," *Progress In Electromagnetics Research M*, Vol. 96, 55–67, 2020.
5. Heath, Jr., R. W., T. Wu, Y. H. Kwon, and A. C. K. Soong, "Multiuser MIMO in distributed antenna systems with out-of-cell interference," *IEEE Transactions on Signal Processing*, Vol. 59, 4885–4899, 2011.
6. Wang, Q., D. Debbarma, A. Lo, Z. Cao, I. Niemegeers, and S. H. D. Groot, "Distributed antenna system for mitigating shadowing effect in 60 GHz WLAN," *Wireless Personal Communications*, Vol. 82, 811–832, 2015.
7. Rasekh, M. E., M. Abdelghany, U. Madhowz, and M. Rodwell, "Phase noise analysis for mmwave massive MIMO: A design framework for scaling via tiled architectures," *Proceedings of the 2019 53rd Annual Conference on Information Sciences and Systems (CISS)*, 1–6, Baltimore, MD, USA, March 2019.
8. Sekiguchi, T., N. Shiga, S. Nakajima, K. Otobe, N. Kuwata, and K. Matsuzaki, H. Hayashi, "Ultra small sized low noise block downconverter module," *Proceedings of the IEEE 1992 Microwave and Millimeter-Wave Monolithic Circuits Symposium Digest of Papers*, 155–158, Albuquerque, NM, USA, 1992.

9. Kamio, K. and T. Sato, "An adaptive sidelobe cancellation algorithm for high-gain antenna arrays," *Electronics and Communications in Japan Part I — Communications*, Vol. 87, 11–18, 2004.
10. Biguesh, M., S. Valaee, B. Champagne, M. H. Bastani, and F. Farzaneh, "A robust sidelobe canceller for reflector antenna using signal subspace eigenvectors," *Revue HF Tijdschrift 2001*, 37–47, 2001.
11. Krichene, H. A., M. T. Ho, S. H. Talisa, G. F. Ricciardi, and K. C. Lauritzen, "Effects of channel mismatch and phase noise on jamming cancellation," *Proceedings of the 2014 IEEE Radar Conference*, 38–43, Cincinnati, OH, USA, May 2014.
12. Zhou, M., Q. Wang, F. He, Y. Zhang, K. Luo, and J. Meng, "Impacts of phase noise on the performance of adaptive side-lobe cancellation system," *Proceedings of the 2021 IEEE 4th International Conference on Electronic Information and Communication Technology (ICEICT)*, 106–109, Xi'an, China, 2021.
13. Schenk, T. C. W., X. J. Tao, P. F. M. Smulders, and E. R. Fledderus, "On the influence of phase noise induced ICI in MIMO OFDM systems," *IEEE Communications Letters*, Vol. 9, 682–684, 2005.
14. Gokceoglu, A. H., Y. Zou, M. Valkama, P. C. Sofotasios, P. Mathecken, and D. Cabric, "Mutual information analysis of OFDM radio link under phase noise, IQ imbalance and frequency-selective fading channel," *IEEE Transactions on Wireless Communications*, Vol. 12, 3048–3059, 2013.
15. Hoefel, R. P. F., "IEEE 802.11ax: On hardware impairments and mitigation schemes for OFDM uplink multi-user MIMO PHY," *Proceedings of the 2018 IEEE 87th Vehicular Technology Conference (VTC Spring)*, 1–5, Porto, June 2018.
16. Pitarokoilis, A., S. K. Mohammed, and E. G. Larsson, "Uplink performance of time-reversal MRC in massive MIMO systems subject to phase noise," *IEEE Transactions on Wireless Communications*, Vol. 14, 711–723, 2015.
17. Pitarokoilis, A., E. Bjornson, and E. G. Larsson, "Performance of the massive MIMO uplink with OFDM and phase noise," *IEEE Communications Letters*, Vol. 20, 1595–1598, 2016.
18. Chatelier, B. and M. Crussiere, "On the impact of phase noise on beamforming performance for mmwave massive MIMO systems," *Proceedings of the 2022 IEEE Wireless Communications and Networking Conference (WCNC)*, 1563–1568, Austin, TX, USA, 2022.
19. Corvaja, R. and A. Garcia-Armada, "Analysis of SVD-based hybrid schemes for massive MIMO with phase noise and imperfect channel estimation," *IEEE Transactions on Vehicular Technology*, Vol. 69, 7325–7338, 2020.
20. Fang, Y., L. Qiu, X. Liang, and C. Ren, "Cell-free Massive MIMO systems with oscillator phase noise: Performance analysis and power control," *IEEE Transactions on Vehicular Technology*, Vol. 70, 10048–10064, 2021.
21. Jin, S.-N., D.-W. Yue, and H. H. Nguyen, "Spectral efficiency of a frequency-selective cell-free massive MIMO system with phase noise," *IEEE Wireless Communications Letters*, Vol. 10, 483–487, 2020.
22. Chen, X., H. Wang, W. Fan, Y. Zou, A. Wolfgang, T. Svensson, and J. Luo, "Phase noise effect on MIMO-OFDM systems with common and independent oscillators," *Wireless Communications and Mobile Computing*, Vol. 2017, 1–12, 2017.
23. Carboun, D. O., R. A. Games, and R. T. Williams, "A principal components sidelobe cancellation algorithm," *Proceedings of the 1990 Conference Record Twenty-Fourth Asilomar Conference on Signals, Systems and Computers*, 763–768, Pacific Grove, CA, USA, 1990.
24. Zhou, M., Q. Wang, F. He, and J. Meng, "Impacts of phase noise on the anti-jamming performance of power inversion algorithm," *Sensors*, Vol. 22, 1–13, 2022.